A&A 597, A13 (2017)
DOI: 10.1051/0004-6361/201629264

Astronomy & Astrophysics

Lyman-α spectral properties of five newly discovered Lyman continuum emitters

A. Verhamme[1], I. Orlitová[2], D. Schaerer[1,3], Y. Izotov[4], G. Worseck[5], T. X. Thuan[6], and N. Guseva[4]

[1] Observatoire de Genève, Université de Genève, 51 Ch. des Maillettes, 1290 Versoix, Switzerland
e-mail: anne.verhamme@unige.ch
[2] Astronomical Institute, Czech Academy of Sciences, Boční II 1401, 141 00 Prague, Czech Republic
[3] CNRS, IRAP, 14 avenue É. Belin, 31400 Toulouse, France
[4] Main Astronomical Observatory, Ukrainian National Academy of Sciences, 27 Zabolotnoho str., 03680 Kyiv, Ukraine
[5] Max-Planck-Institut für Astronomie, Königstuhl 17, 69117 Heidelberg, Germany
[6] Astronomy Department, University of Virginia, PO Box 400325, Charlottesville, VA 22904-4325, USA

Received 7 July 2016 / Accepted 11 September 2016

ABSTRACT

Aims. We have recently reported the discovery of five low redshift Lyman continuum (LyC) emitters (LCEs) with absolute escape fractions $f_{\rm esc}^{\rm LyC}$ that range from 6 to 13%, higher than previously found and that more than double the number of low redshift LCEs. We use these observations to test theoretical predictions about a link between the characteristics of the Lyman-alpha (Lyα) line from galaxies and the escape of ionizing photons.

Methods. We analyse the Lyα spectra of eight LCEs of the local Universe observed with the Cosmic Origins Spectrograph onboard the *Hubble* Space Telescope (our five leakers and three galaxies from the litterature), and compare their strengths and shapes to the theoretical criteria and comparison samples of local galaxies: the Lyman Alpha Reference Survey, Lyman-break analogs, Green Peas, and the high-redshift strong LyC leaker *Ion2*.

Results. Our LCEs are found to be strong Lyα emitters, with high equivalent widths, EW(Lyα) > 70 Å, and large Lyα escape fractions, $f_{\rm esc}^{\rm Ly\alpha} > 20\%$. The Ly$\alpha$ profiles are all double-peaked with a small peak separation, in agreement with our theoretical expectations. They also have no underlying absorption at the Lyα position. All these characteristics are very different from the Lyα properties of typical star-forming galaxies of the local Universe. A subset of the comparison samples (2−3 Green Pea galaxies) share these extreme values, indicating that they could also be leaking. We also find a strong correlation between the star formation rate surface density and the escape fraction of ionizing photons, indicating that the compactness of star-forming regions plays a role in shaping low column density paths in the interstellar medium of LCEs.

Conclusions. The Lyα properties of LCEs are peculiar: Lyα can be used as a reliable tracer of LyC escape from galaxies, complementing other indirect diagnostics proposed in the literature.

Key words. radiative transfer – dark ages, reionization, first stars – galaxies: ISM – ISM: structure – ISM: kinematics and dynamics – ultraviolet: galaxies

1. Introduction

Cosmic reionization is a major event in the history of the Universe thar took place during the first billion years: after the dark ages, the first sources of light released ionizing radiation in the intergalactic medium, reheating the gas, and changing its opacity. This cosmic feedback of the first astrophysical objects is thought to have influenced the formation and evolution of galaxies in their first stages (Ocvirk et al. 2016) and determines their detectability (Stark et al. 2011; Schenker et al. 2014; Dijkstra 2014, 2016). The open question in current studies of cosmic reionization is to understand the relative contribution of the two types of sources likely involved: quasars and star-forming galaxies. Quasars inject a copious amount of ionizing photons into the intergalactic medium (IGM), but were thought to be too rare at high redshift to have contributed significantly (Fontanot et al. 2012, 2014). A new population of faint active galactive nuclei (AGNs) has been recently reported (Giallongo et al. 2015), which may sustain reionization, assuming that their escape fraction of ionizing photons is high (e.g. 100% in Madau & Haardt 2015). The escape fraction of ionizing photons from AGNs needs to be investigated in more details; recent measurements report much lower values than assumed in previous studies (Micheva et al. 2016).

Our present study focuses on the second type of sources of the cosmic reionization: massive stars in galaxies. As for AGNs, the main uncertainty in quantifying the role of star formation in the cosmic reionization is the escape fraction of ionizing photons from galaxies. Young and massive stars produce ionizing radiation in situ. The difficult question is to observe, measure, and quantify how many of these photons, if any, escape the interstellar medium (ISM) of galaxies. So far, one clear detection has been reported at high redshift, with a high Lyman continuum absolute escape fraction ($f_{\rm esc}^{\rm LyC} > 50\%$ Vanzella et al. 2016b; de Barros et al. 2016), another Lyman continuum emitter (LCE) was recently reported at $z = 3.15$ by Shapley et al. (2016), and a few low-redshift detections with low escape fractions (<5%) have been found during the last decade (Bergvall et al. 2006; Leitet et al. 2013; Borthakur et al. 2014; Leitherer et al. 2016; Puschnig et al. 2016). Significant progress at low redshifts has recently been achieved with the COS spectrograph onboard the

Hubble Space Telescope (HST) by Izotov et al. (2016a,b), who found five LCEs at $z \sim 0.3$ with $f_{\rm esc}^{\rm LyC} \sim 6-13\%$. These sources are the basis of the present study.

Given the extremely low success rate of observational searches for LCEs, several pre-selection methods for good LCE candidates have been proposed, involving the alteration of nebular emission line strengths (Zackrisson et al. 2013), high [O III]/[O II] ratios that potentially trace density-bounded H II regions (Jaskot & Oey 2013; Nakajima & Ouchi 2014), or the non-saturation of the metallic low-ionization absorption lines (Heckman et al. 2011; Alexandroff et al. 2015; Vasei et al. 2016) that trace a low covering fraction of the absorbing gas along the line of sight. We recently proposed a method based on the Lyman-alpha (Lyα) spectral shape of LCEs: strong and narrow Lyα profiles with a shift of the main peak smaller than $\sim$150 km s^{-1}, or double peaks closer than $\sim$300 km s^{-1} may indicate LyC leakage (see Verhamme et al. 2015, for more details). Now is the time to test these simple predictions.

In this work, we assess the specificity of the Lyα properties of LCEs by comparing them to other samples of low-redshift star-forming galaxies whose Lyα properties have been measured and analysed: the Lyman Alpha Reference Survey (LARS), Lyman-break analogs (LBAs), and Green Pea galaxies (GPs). The LARS sample consists of 14 star-forming galaxies at redshifts $z = 0.02-0.2$. They were selected from the cross-matched SDSS and GALEX catalogues to sample the range of far-UV luminosities observed in $z \sim 3$ Lyman break galaxies (LBGs). Only galaxies with active star formation were included, requiring EW(Ha) > 100 Å. The aim of LARS is to study the mechanisms governing Lyα escape from galaxies (see Östlin et al. 2014, for an overview). Most LARS galaxies are dwarf irregulars. LARS14 is also a GP (see below).

The LBAs were selected from the GALEX catalogue for their far-UV luminosity, high surface brightness, and compactness (Heckman et al. 2005). They resemble high-redshift LBGs in physical size, stellar mass, star-formation rate, metallicity, dust extinction, and gas velocity dispersion. UV and optical morphologies of 30 LBAs have been studied by Overzier et al. (2009). The UV shows massive star-forming clumps, while evidence of interaction is seen in the optical images. In 20% of the sample, all of the UV light comes from a single, compact star-forming clump, usually characterised by strong outflows. Far-UV spectra of 22 LBAs were obtained with HST/COS (Heckman et al. 2011; Alexandroff et al. 2015). Most of their Lyα lines are observed in emission, with a variety of profiles including P-Cygni, as well as broad and narrow double-peaks. The escape of ionizing photons from one LBA, J0921+4509, was reported in Borthakur et al. (2014), with an absolute escape fraction of 1%. The probability of LyC leakage from the other LBAs was discussed in Alexandroff et al. (2015) by comparing the indirect diagnostics for LyC escape discussed above.

Green Pea galaxies were noticed in the Galaxy Zoo SDSS images for their bright green colour and compactness. The colour is due to strong [O III]λ5007 Å emission, which reaches equivalent widths as high as 1000 Å. Cardamone et al. (2009) identified a sample of ~250 GPs in SDSS DR7, at $z = 0.11-0.36$, while Izotov et al. (2011) extended the number to ~800 over a larger redshift range $z = 0.02-0.63$ (the colour changes with redshift, but their properties remain similar). GPs share many properties with high-redshift LBGs and Lyman alpha emitters (LAEs). Twelve archival HST/COS spectra of GPs (outside our sample) are available (Henry et al. 2015; Yang et al. 2016), drawn from Cardamone et al. (2009). They are all strong Lyα emitters, most of which have double-peaked line profiles. The escape of ionizing photons from GPs was discussed on the basis of their Lyα spectral shapes (Verhamme et al. 2015). Some are best fitted by synthetic Lyα spectra emergent from low column density geometries, indicating that they could be leaking (Yang et al. 2016; Orlitova et al., in prep.).

As reported in Izotov et al. (2016a,b), we detected LyC emission from five compact, strongly star-forming galaxies of the local Universe, with high [O III]/[O II] ratios (>4). These galaxies belong to the GP category. To our knowledge, this was the first attempt to test if high [O III]/[O II] ratios are linked to LyC leakage. The major result of this study has been to discover that five out of the five observed objects are leaking ionizing radiation, and the finding of a correlation between $f_{\rm esc}^{\rm LyC}$ and [O III]/[O II] (see Fig. 14 in Izotov et al. 2016b). Therefore, a high [O III]/[O II] ratio appears as a potential signature of LyC escape. Since nothing was known about Lyα for these galaxies, it is interesting to study the Lyα properties of these LCEs and to use these sources to test our theoretical predictions in relation to LyC leakage, Lyα escape, and the detailed Lyα line profiles (Verhamme et al. 2015). This is the main objective of this paper.

In Sect. 2, we describe the observational data used in our study. In Sect. 3, we discuss the Lyα properties of LCEs and comparison samples, showing that LCEs have a strong Lyα emission. We then present and discuss the detailed Lyα line profiles of these galaxies (Sect. 4). The results are briefly put into perspective and discussed in Sect. 5. Our main conclusions are summarised in Sect. 6.

2. Description of the data

2.1. Lyman continuum leakers

We use Lyα observations of all known low redshift LCEs, combining data from five objects that have recently been reported by our team (Izotov et al. 2016a,b) and three other sources from the literature. The Lyα spectra of our LCEs were observed with HST/COS using two gratings: the medium resolution G160M grating, and the low-resolution G140L grating (GO 13744, PI: T.X.Thuan). The data were reduced with custom software specifically designed for faint HST/COS targets (Worseck et al. 2011; Syphers et al. 2012), as described in Izotov et al. (2016a,b). For Lyα and other parts of the spectrum with strong fluxes, our custom reduction yields results that are equivalent to those of the standard COS pipeline. To this we add the other three low redshift objects that have a direct detection in the Lyman continuum and whose Lyα spectra have also been observed with COS. Haro 11 is a known LyC leaker of the local Universe, with an absolute escape fraction $f_{\rm esc}^{\rm LyC} \sim 3\%$ (Leitet et al. 2011, 2013), its Lyα spectrum has been observed with the G130M grating (GO13017, PI: T. Heckman) and discussed in Alexandroff et al. (2015) and Verhamme et al. (2015). Tololo 1247-232 has $f_{\rm esc}^{\rm LyC} \sim 4-6\%$ (Leitet et al. 2013; Leitherer et al. 2016; Puschnig et al., priv. comm.) and its Lyα spectrum was observed with G130M (GO13027, PI: G. Ostlin, Puschnig et al., priv. comm.). Ionizing flux has also been detected from the LBA J0921+4509, with $f_{\rm esc}^{\rm LyC} \sim 1\%$ (Borthakur et al. 2014), and its Lyα spectrum has also been observed with G130M (GO11727, PI: T. Heckman, Heckman et al. 2011; Verhamme et al. 2015; Alexandroff et al. 2015). The COS observations of the three sources from the literature were retrieved from the MAST archive, reduced with the up-to-date version of the standard COS pipeline.

Table 1. Measured Lyα and other related properties of all known low-z LCEs, ordered by decreasing f_{esc}^{LyC} (8th column).

ID	EW(Lyα) Å	$f_{esc}^{Lyα}$	V_{peak}^{blue} km s^{-1}	V_{peak}^{red} km s^{-1}	V_{sep} km s^{-1}	EW_{blue}/EW_{red}	f_{esc}^{LyC}	[O III]/[O II]	Σ_{SFR} $M_\odot$ yr^{-1} kpc^{-2}
J1152+3400	79	0.36	−120	150	270	0.55	0.132	5.4	35.5
J1442−0209	129	0.57	−250	60	310	0.17	0.074	6.7	15.5
J0925+1403	83	0.31	−160	150	310	0.40	0.072	4.8	12.6
J1503+3644	98	0.31	−290	140	430	0.17	0.058	4.9	6.8
J1333+6246	75	0.55	−300	90	390	0.10	0.056	4.8	2.2
Tol 1247-232	29	0.20	−300	150	450	0.12	0.045	3.4	
Haro11	15	0.04	−300	110	410	0.06	0.032	1.5	1.1
J0921+4509	4	0.01	−450	240	690	1.0	0.01	0.3	7.9

Notes. The Lyα equivalent width, EW(Lyα), is given in the rest-frame. The EW uncertainties are estimated as ±20 Å. The last column contains the star formation rate per unit area, Σ_{SFR}, in $M_\odot$ yr^{-1} kpc^{-2}. Columns 2, and 8−10 are taken from Izotov et al. (2016a,b). Note that $f_{esc}^{Lyα}$ has been recalculated from Izotov et al. (2016a,b), without SDSS vs. COS aperture correction, for comparison with other samples (see text for more details). The typical uncertainties on velocity shift measurements are ±10 km s^{-1} (see text for more details).

All spectra were binned in the same way, and the following quantities were measured in a homogeneous manner: the Lyα equivalent width, EW(Lyα), the location of local maxima in the profiles, V_{peak}^{blue} for the maximum blueward of the systemic redshift, and V_{peak}^{red} for the maximum on the red side. We also measure the separation between the red and blue peaks

$$V_{sep} = V_{peak}^{red} - V_{peak}^{blue}. \quad (1)$$

The measurements for all LCEs are summarised in Table 1. The effective spectral resolution of the spectra is $R \sim 4000$, as estimated by convolving the observed spectrum with Gaussians to mimic the effect of the line spread function on the data.

These measurements are affected by spectral resolution, as demonstrated later, but maybe also by sampling the data, the continuum determination, and the redshift accuracy. Since our galaxies are in the SDSS database, the data for several strong optical nebular lines are available, enabling a very precise systemic redshift measurement (<15 km s^{-1}, for a typical spectral resolution of $R \sim 2000$ in SDSS). The main uncertainty on velocity shift measurements comes from COS wavelength calibration, which we estimate at ±40 km s^{-1}, following the detailed discussion in Henry et al. (2015). The Lyα sizes of galaxies are usually bigger than their UV size (Steidel et al. 2011; Hayes et al. 2013). COS resolution decreases with the extent of the source inside the aperture, so the effective spectral resolution around Lyα is probably lower than in the continuum. We binned the data to increase the signal to noise, keeping ∼5 resolution elements in the main component of the profile, i.e. the red peak. We also checked that different binnings lead to velocity shifts that are much lower than the wavelength calibration uncertainties, $\Delta V \sim \pm 10$ km s^{-1}. We measured the continuum level from two different methods (local estimation vs. global fit). The difference in EW measurements computed from these two continuum estimates is typically ±20 Å, which we assume to be the typical uncertainty in our EW measurements.

The Lyα escape fractions, reported in Table 1, were calculated from the Balmer lines in the SDSS spectra for our five LCEs by Izotov et al. (2016b) and J0921+04509, by the equation

$$f_{esc}^{Lyα} = F(\mathrm{Ly}\alpha)/(8.2 \times F(\mathrm{H}\alpha)_{corr}), \quad (2)$$

where F(Lyα) is the observed Lyα flux, and $F(\mathrm{H}\alpha)_{corr}$ the Hα flux corrected for internal extinction. Both Lyα and Hα are corrected for the foreground Milky Way extinction. We assumed an intrinsic factor of 8.2 between the intrinsicLyα and Hα fluxes (Dopita & Sutherland 2003). We could use the Hα SDSS data because the SDSS aperture is of similar size of the HST/COS spectrograph (2.5″ for COS and 3″ for SDSS). In contrast with the measures reported in Izotov et al. (2016a,b), we do not apply any aperture correction here. We compute $f_{esc}^{Lyα}$ from our LCEs, in the same way as in other studies, to compare this with values reported in the literature, and with GPs in particular. Therefore our $f_{esc}^{Lyα}$ values are larger by a factor of 1.4 compared to those reported in Izotov et al. (2016a,b). The two other LCEs Haro 11 and Tol 1247-232 are not in the SDSS database, so $f_{esc}^{Lyα}$ are derived from imaging and not spectroscopy, and are integrated $f_{esc}^{Lyα}$ measurements (as for LARS) and not limited to the COS aperture. For Haro 11, Östlin et al. (2009) obtained $f_{esc}^{Lyα} = 0.037$ from Lyα and Hα images. A value of $f_{esc}^{Lyα} = 0.20$ was derived by Puschnig et al. (priv. comm.) for Tol 1247-232 from HST imaging and COS spectroscopy.

2.2. Comparison samples

Subsequently we compare our measurements with the Lyα properties of two other samples of local galaxies that have been discussed in the context of LyC leakage from galaxies, the GPs, and LBAs. In practice we have been able to compile measurements for 12 GPs (Jaskot & Oey 2014; Henry et al. 2015; Yang et al. 2016), and eight LBAs (Heckman et al. 2011). The Lyα measurements are taken from these papers and from Verhamme et al. (2015). For comparison with normal low redshift star-forming galaxies, we also use Lyα data of the 14 LARS galaxies reported in Hayes et al. (2013, 2014), Rivera-Thorsen et al. (2015). In particular, the LARS EW(Lyα) and $f_{esc}^{Lyα}$ reported in Fig. 1 are global measurements, derived from Lyα and Hα imaging, taken from Hayes et al. (2014). The LARS, LBA, and GP samples were briefly discussed above (Sect. 1). Finally, we also include the confirmed $z = 3.218$ Lyman continuum leaker *Ion2* from Vanzella et al. (2015), de Barros et al. (2016), and Vanzella et al. (2016b) for comparison. From these papers, *Ion2* has EW(Lyα) ∼ 94 Å, $f_{esc}^{LyC} \sim 0.64$, $f_{esc}^{Lyα} > 0.78$, [O III]/[O II] > 10, and a SFR density $\Sigma_{SFR} \sim 43$ $M_\odot$ yr^{-1} kpc^{-2}.

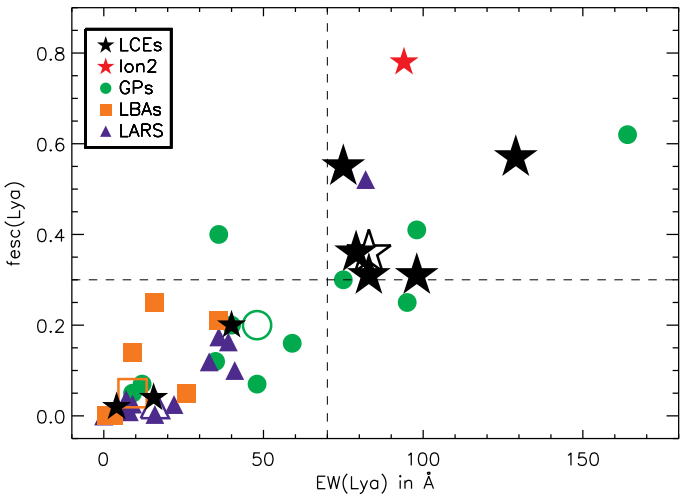

Fig. 1. Comparison of two measures of the Lyα strength, $f_{\rm esc}^{\rm Ly\alpha}$ and EW(Lyα), of LCEs with that of GPs, LBAs, and LARS: strong LCEs, shown by large black stars, are more extreme than the comparison samples. The open symbols show the median of the distributions for each sample. The red star shows the location of the high-redshift strong LyC leaker *Ion2*. The dashed lines delimit the upper right panel containing all strong LyC leakers.

3. LCEs have strong Lyα emission

In Fig. 1 we plot the Lyα equivalent width EW(Lyα) of the eight low-redshift LCEs from Table 1, as well as the high-z LCE *Ion2* (star symbols) as a function of $f_{\rm esc}^{\rm Ly\alpha}$. The comparison samples, including GPs, LBAs, and the LARS sources are also shown. Clearly, the five compact LCEs from Izotov et al. (2016a) and Izotov et al. (2016b) fall in the upper right corner of the plot: they have $f_{\rm esc}^{\rm Ly\alpha} > 30\%$ and EW(Lyα) > 70 Å. These are extreme values for galaxies in the local Universe, very different from the distribution of EW(Lyα) for LARS and LBAs, whose median values are shown by the large open symbols. Only some GPs (and one LARS object, LARS02) fall into the same region of the plot, and their median value is higher. *Ion2* (red star), the strong LyC leaker of the high-z Universe (de Barros et al. 2016; Vanzella et al. 2016b), also falls into the same region.

As shown by the open black star, the median values of our five LCEs are $f_{\rm esc}^{\rm Ly\alpha} = 0.36$ and EW(Lyα) = 83 Å for a median $f_{\rm esc}^{\rm LyC} = 0.07$. So, empirically, we deduce from Fig. 1 that LCEs with $f_{\rm esc}^{\rm LyC} > 5\%$ have a high $f_{\rm esc}^{\rm Ly\alpha}$(>0.30) and a high EW (>70 Å). However, whether the reverse is also true, i.e. if all galaxies with high $f_{\rm esc}^{\rm Ly\alpha}$ and high EW(Lyα) are also leaking ionizing photons, remains to be examined. Theoretically, all dust-free systems have an angle-averaged $f_{\rm esc}^{\rm Ly\alpha} = 1$, since Ly$\alpha$ photons are only scattered and not destroyed by interactions with hydrogen, independently of their LyC optical depth. Galaxies with a high observed Lyα equivalent width but a low $f_{\rm esc}^{\rm Ly\alpha}$ (i.e. in the lower right corner of Fig. 1) are not expected, since this would imply a very large intrinsic EW(Lyα), whereas a maximum EW(Lyα) $\approx$ 240 Å is expected for very young, normal stellar populations (Schaerer 2003).

We now investigate direct correlations between $f_{\rm esc}^{\rm LyC}$ and the two indicators of strength of the Lyα emission, EW(Lyα) and $f_{\rm esc}^{\rm Ly\alpha}$, for the LCE sample. In the left panel of Fig. 2, we find a trend between EW(Lyα) and $f_{\rm esc}^{\rm LyC}$: galaxies with higher $f_{\rm esc}^{\rm LyC}$have higher EW(Lya). Part of this observed trend could be due to selection effects, since the LCEs from our team (black stars) were selected for their strong emission lines in the optical (among other criteria) to search for sources with an intrinsically strong Lyman continuum flux. In principle, sources with faint emission lines, e.g. at the advanced stage after a burst of star formation, could have an ISM allowing the escape of LyC photons, which would correspond to sources with a low EW(Lyα) and arbitrary values of $f_{\rm esc}^{\rm LyC}$. Whether such sources exist in nature cannot presently be excluded. However, their contribution to cosmic reionization would probably be insignificant, since they would have a low LyC photon production. In other words, it seems more likely that sources of relevance for cosmic reionization, say with $f_{\rm esc}^{\rm LyC} \gtrsim 5\%$, also show a high Ly$\alpha$ equivalent width, as the sources in Fig. 2 show.

For a given intrinsic Lyα equivalent width of the population, $EW_{\rm int}$(Lyα), the observed EW(Lyα), and $f_{\rm esc}^{\rm LyC}$ are linked by the equation

$$EW(\mathrm{Ly}\alpha) = EW_{\rm int}(\mathrm{Ly}\alpha) \times (1 - f_{\rm esc}^{\rm LyC}) \times f_{\rm esc}^{\rm Ly\alpha} / f_{\rm esc}^{\rm UV}, \quad (3)$$

where $f_{\rm esc}^{\rm UV}$ is the escape fraction of the non-ionizing, non-resonant UV continuum around Lyα, and $f_{\rm esc}^{\rm Ly\alpha}$ is as before. For two maximum values of intrinsic Lyα emission limits with $EW_{\rm int}$(Lyα) = 240 and 80 Å respectively, corresponding to a young metal-poor burst and constant star-formation (cf. Schaerer 2003), the dashed lines in Fig. 2 show the corresponding maximum observed EW(Lyα) assuming $f_{\rm esc}^{\rm Ly\alpha} = f_{\rm esc}^{\rm UV}$. This assumption implies that Lyα photons are destroyed by dust in the same proportion as the UV non-resonant radiation, as observed for at least some local LAEs (Atek et al. 2014; Henry et al. 2015). This shows that observed EWs of the strong LCEs are within the expected range. Only for very high values of the Lyman continuum escape ($f_{\rm esc}^{\rm LyC} \gtrsim 0.5$) does the expected Ly$\alpha$ strength also decrease due to a significant loss of ionizing photons, as illustrated by the decrease of the dashed lines in Fig. 2 (see also Fig. 13 in Nakajima & Ouchi 2014). The dotted lines in Fig. 2 show the same, but for $f_{\rm esc}^{\rm Ly\alpha} = 0.1 f_{\rm esc}^{\rm UV}$, i.e. when Ly$\alpha$ photons are more destroyed by dust than by UV continuum photons. This effect, observed in many star-forming galaxies (e.g. Atek et al. 2008, 2014), is one possible explanation for the low EW(Lyα) observed in three of the low-z LCEs.

In the right panel of Fig. 2, we show $f_{\rm esc}^{\rm Ly\alpha}$ as a function of $f_{\rm esc}^{\rm LyC}$, which are found to correlate for the eight LCEs and *Ion2*. As the dashed line that indicates the one-to-one relation shows, the Lyα escape fraction is generally higher than the Lyman continuum escape fraction, typically ~2−10 times higher for this set of data, except for Haro11. This result can be explained as follows: the escape of ionizing photons from galaxies is only possible when the amount of neutral gas along the line of sight is particularly low ($\log(N_{\rm HI} < 1.6 \times 10^{17}$ cm^{-2}), at least over a partial area of the galaxy in front of star-forming regions. Furthermore, this peculiar geometrical configuration is also extremely favourable to Lyα escape (Behrens et al. 2014; Verhamme et al. 2015), so that Lyα photons can preferentially escape along these low column density channels. The reason why $f_{\rm esc}^{\rm Ly\alpha}$ is expected to be higher than $f_{\rm esc}^{\rm LyC}$ is due to the resonant nature of the line: thanks to scattering, some Lyα photons that were not emitted in front of a hole can be scattered into a clear line of sight, so that more Lyα photons find holes compared to the non-resonant LyC photons. Therefore, LCEs are expected to have a high $f_{\rm esc}^{\rm Ly\alpha}$ and $f_{\rm esc}^{\rm Ly\alpha} / f_{\rm esc}^{\rm LyC} > 1$. If our empirical result holds more universally, it implies that objects with $f_{\rm esc}^{\rm LyC} > 10\%$ should have at

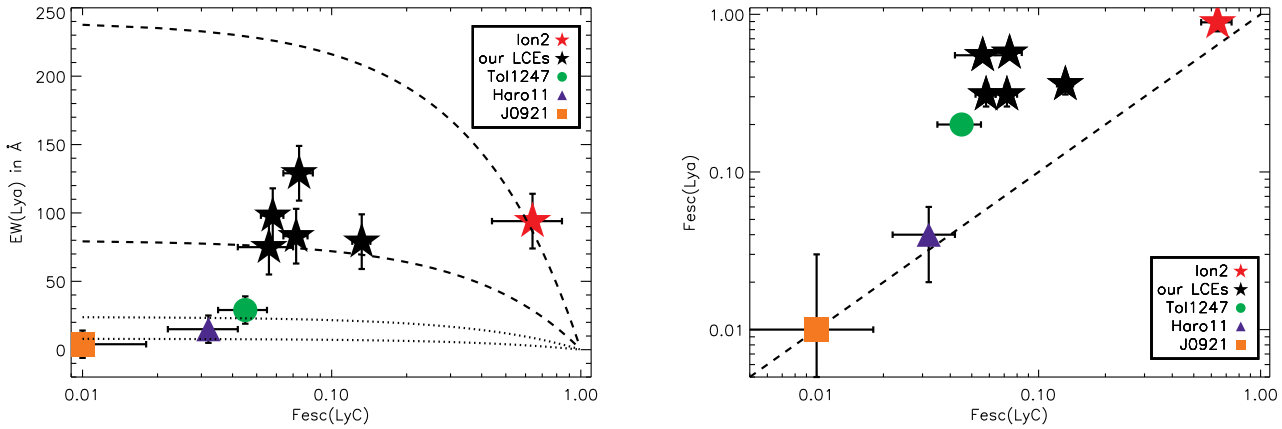

Fig. 2. Lyα strength versus the escape of ionizing photons from eight galaxies of the local Universe: our five leakers (Izotov et al. 2016a,b), the LBA J0921+4509 (Borthakur et al. 2014), Haro11 and Tol1247(Leitherer et al. 2016), and the high redshift galaxy *Ion2* (de Barros et al. 2016; Vanzella et al. 2016b). *Left*: the Lyα EWs of LCEs seem to correlate with the escape fraction of ionizing photons. The dashed lines show theoretical predictions for the same attenuation in the Lyα line as in the continuum, for an instantaneous burst (upper curve) or a constant star formation history (lower curve). The dotted lines are the same but, for Lyα, ten times more extinguished than the continuum. See text for more details. *Right*: $f_{\rm esc}^{\rm Ly\alpha}$ correlates with $f_{\rm esc}^{\rm LyC}$, and is generally larger than $f_{\rm esc}^{\rm LyC}$. The dashed line shows the one-to-one relation.

least $f_{\rm esc}^{\rm Ly\alpha} > 20\%$. Larger samples will be needed to firm up this result.

Regarding the observed relation between $f_{\rm esc}^{\rm Ly\alpha}$ and $f_{\rm esc}^{\rm LyC}$ we also note that theoretical predictions from clumpy geometries presented by Dijkstra et al. (2016) show the same trend of $f_{\rm esc}^{\rm Ly\alpha} > f_{\rm esc}^{\rm LyC}$, albeit with a much larger scatter in the ratio $f_{\rm esc}^{\rm Ly\alpha}/f_{\rm esc}^{\rm LyC}$ than observed here. However, their predicted escape fractions correspond to averages over all angles, i.e. global escape fractions, which are not directly comparable to observations. Finally, we have searched the literature for other samples providing measurements (or upper limits) of both $f_{\rm esc}^{\rm Ly\alpha}$ and $f_{\rm esc}^{\rm LyC}$. The few studies/surveys providing this data (e.g. $z \sim 2$ Hα emitters, Matthee et al. 2016b,a) are compatible with the relation between $f_{\rm esc}^{\rm Ly\alpha}$ and $f_{\rm esc}^{\rm LyC}$ followed by the LCEs studied here. In particular, no strong LCE with a low Lyα escape fraction is known, nor do we know of sources with a high $f_{\rm esc}^{\rm Ly\alpha}$ and a stringent LyC detection limit.

We conclude that the current data shown in both panels of Fig. 2 strongly suggest that strong LCEs should be found among galaxy samples with strong Lyα emission, characterised by a high equivalent width (EW(Lyα) $\gtrsim 70$ Å), and/or a high Lyα escape fraction. We now examine the detailed Lyα line profiles of the LCEs.

4. LCEs have narrow double-peaked Lyα profile

In Figs. 3 and 4 we present the Lyα line profiles of the five strong LCEs, ordered from top to bottom by decreasing $f_{\rm esc}^{\rm LyC}$. Once again, the fact that they are all strong Lyα emitters is very different from the typical low-redshift Lyα profiles from galaxies studied so far (Wofford et al. 2013; Rivera-Thorsen et al. 2015), except for some of the GPs (Jaskot & Oey 2014; Henry et al. 2015) and some LBAs (Heckman et al. 2011; Alexandroff et al. 2015). Our objects show two remarkable features, illustrated in the figure. First, it shows strong and narrow lines which are all double-peaked, by which we mean Lyα profiles with two maxima on each side of the systemic redshift. Second, the profile of the strong leakers never falls below the continuum level. We now quantify and discuss these features and compare them to other objects.

4.1. Properties of the double-peaked profiles

As just mentioned, all Lyα profiles shown here exhibit two peaks, one blueward and one redward of the systemic redshift. This feature, more specifically the ratio between the EW of the blue component to the red one (Col. 7 in Table 1), has been proposed as an empirical diagnostics for LyC leakage (Erb et al. 2014; Alexandroff et al. 2015). The presence of a blue peak can be understood as a low column density effect. The classical Lyα P-Cygni profiles emerging from galaxies present a blueshifted absorption, similar to the absorption profiles of low ionization state (LIS) metallic lines. This is due to outflowing neutral gas along the line of sight: the blue photons are seen at resonance for this scattering medium, they are absorbed in the blue and scattered away from resonance (the red peak emerges because most photons have already been emitted to the red for the scattering medium). It seems that in LCEs, it is possible for photons to escape when there is a blue frequency, meaning that the optical depth of the intervening medium is low enough to allow their escape. We can think of two different scenarios: in a homogeneous medium, both the column density and the velocity of the neutral gas have to be low to shape double peaks with small separations, but a clumpy outflowing medium can also shape double peaks, as proposed and studied in detail in Gronke & Dijkstra (2016). To get an insight into the geometry and the kinematics of the intervening neutral gas, we are currently investigating the LIS metallic absorption profiles (Orlitova et al., in prep.).

In Fig. 5, we present the peak shift measurements versus the escape fraction of ionizing photons for all objects of Table 1. A clear anti-correlation is found between the escape fraction of ionizing photons and the separation of the peaks in the Lyα profile (first panel) decreasing to $V_{\rm sep} \sim 300$ km s^{-1} for the highest $f_{\rm esc}^{\rm LyC}$. Along the same lines, Hashimoto et al. (2015) showed that the peaks separation is lower, and the velocity shift of the red peak is smaller, in a sample of $z \sim 2.2$ LAEs than typically measured in LBGs (Shapley et al. 2003; Kulas et al. 2012), in correlation with lower $N_{\rm HI}$ estimates for LAEs than for LBGs from Lyα line profile fitting (Hashimoto et al. 2015, their Fig. 11). As predicted by radiation transfer modelling in idealised geometries (Verhamme et al. 2015), the width and the shift of the main peak or the peak separation trace the column density of the scattering

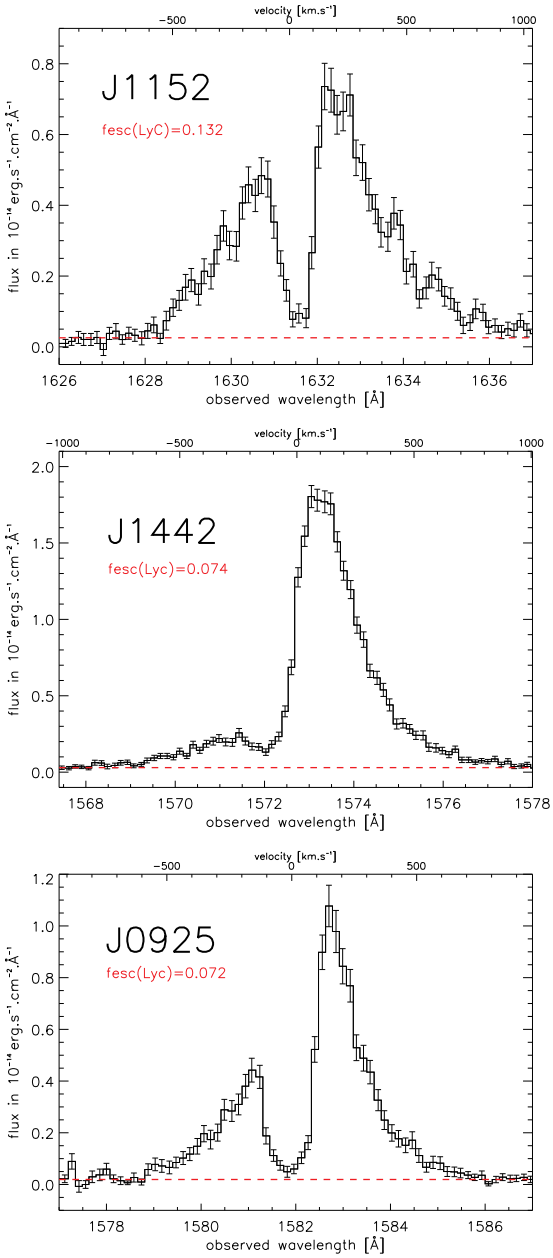

Fig. 3. Lyα line shapes of LCEs. The whole G160M Lyα profiles are shown over a small wavelength range, ordered by decreasing $f_{\rm esc}^{\rm LyC}$ *from top to bottom*. They all have very peculiar double peaked profiles, with small peak separation. The dashed lines show the continuum level determined from the entire G160M spectra.

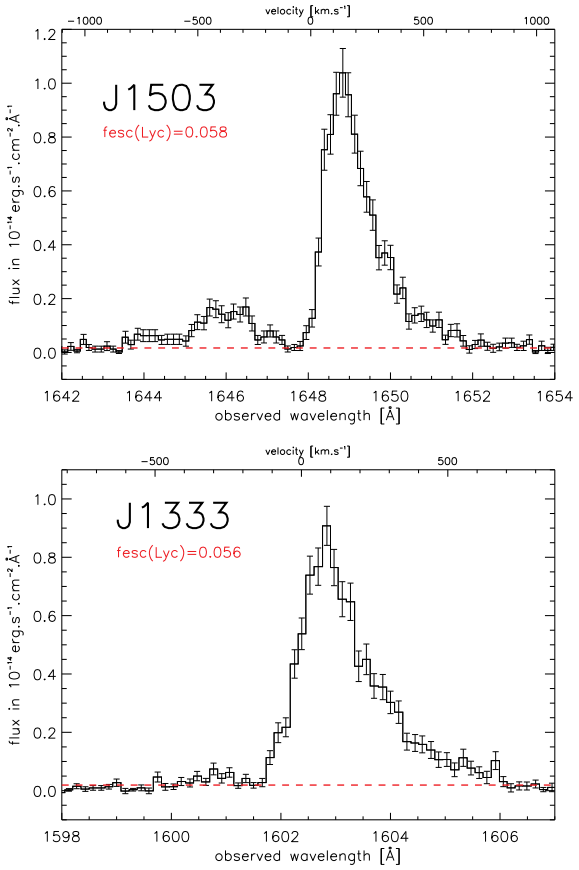

Fig. 4. Same as Fig. 3 for the remaining two sources.

medium. In particular, a peak separation of ~300 km s^{-1} and smaller corresponds to Lyα radiation transfer in media with column densities below $N_{\rm HI} = 1.6 \times 10^{17}$ cm^{-2}. Our predictions were made for media with an optical depth of $\tau_{\rm LyC} \sim 1$ for the ionizing radiation, corresponding to an escape fraction of ~30%, higher than observed in our sample, but these characteristic signatures seem to hold even at lower escape fractions. Indeed, our five LCEs all have small peak separations, although slightly higher than the predicted 300 km s^{-1} value, as reported in Table 1. Knowing $f_{\rm esc}^{\rm LyC}$ for our objects, we can estimate the column density of neutral gas along the line of sight corresponding to their LyC escape fractions:

$$N_{\rm HI} = -\ln(f_{\rm esc}^{\rm LyC})/\sigma_0, \quad (4)$$

where $\sigma_0 = 6.3 \times 10^{-18}$ cm^2. This corresponds to $N_{\rm HI} = (3.2\text{–}4.6) \times 10^{17}$ cm^{-2} for our LCEs. So the anti-correlation between $f_{\rm esc}^{\rm LyC}$ and $V_{\rm sep}$ discussed above translates into an anti-correlation between $N_{\rm HI}$ and $V_{\rm sep}$.

Interestingly in our data, the behaviour of $V_{\rm sep}$ is not driven by the location of the red peak (third panel), but by the blue one (second panel). Henry et al. (2015) already report the strongest correlation between the shift of the blue peak, $V_{\rm peak}^{\rm blue}$, and $f_{\rm esc}^{\rm Ly\alpha}$ for GPs; we also find the strongest correlation between $V_{\rm peak}^{\rm blue}$ and $f_{\rm esc}^{\rm LyC}$. In the case of *Ion2*, with current lower spectral resolution data, the blue peak is consistent with systemic redshift (see Table 1 in de Barros et al. 2016) and $f_{\rm esc}^{\rm LyC}$ is very high (>50%), so *Ion2* would also follow the reported trend. In fact the location of the red peak is very close to or below the theoretical prediction for LyC leakage ($V_{\rm peak}^{\rm red} < 150$ km s^{-1}) and almost the same for seven out of eight objects. Only the LBA J0921+4509 has clearly higher peak offsets so no trend is seen between the escape fraction of ionizing photons and the red peak location. A (very) small velocity shift of the main peak rather appears as a necessary condition for LyC escape. But the location of the blue peak seems to correlate more strongly with the escape of ionizing photons. A stronger trend with the blue peak compared to the red peak was not predicted by our models. Further theoretical work needs to be done to understand this observational trend, clumpiness appearing as an interesting geometry to explore (Gronke & Dijkstra 2016).

As already mentioned, the ratio of the EWs of the blue and the red peaks has been proposed as a empirical criterion for LyC escape, because it seems to correlate with the depth of the LIS lines (Erb et al. 2014; Alexandroff et al. 2015). We

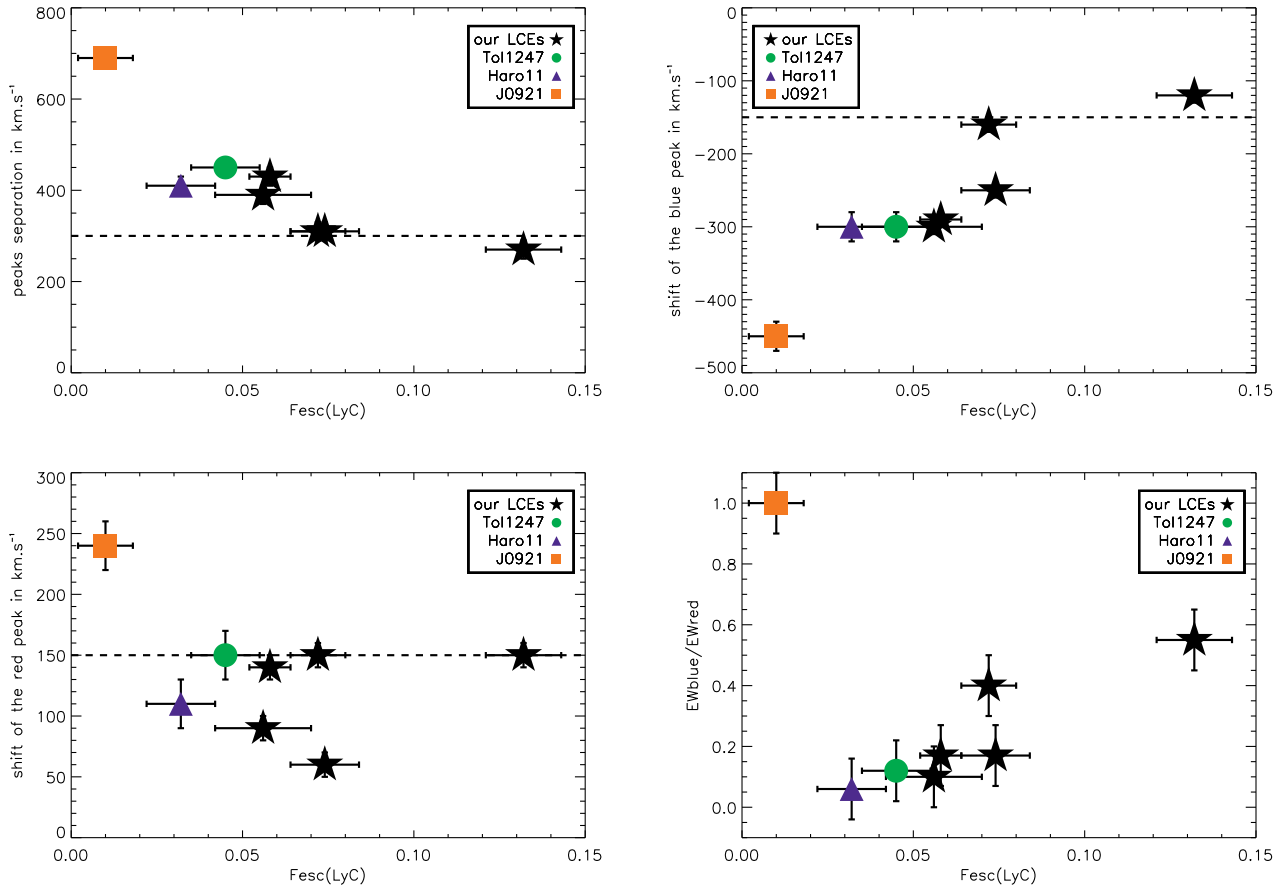

Fig. 5. Comparison of the Lyα diagnostics for LyC leakage with the escape fraction of ionizing photons. The correlation between the peak separation and the escape fraction of ionizing photons is driven by the shift of the blue peak back to line center. The dashed lines correspond to the theoretical predictions for $f_{\rm esc}^{\rm LyC} \sim 30\%$ ($\tau_{\rm LyC} \sim 1$) from Verhamme et al. (2015).

investigate this correlation in the fourth panel of Fig. 5, but the trend appears less clear than for the peak separation, or the blue peak shift: our strongest leaker J1152+3400 has a prominent blue peak, but the object with the lower escape fraction, LBA J0921+4509, too. The second strongest leaker, J1442−0209, has just a small blue bump, but the whole profile is clearly in emission. There is no clear theoretical support to this criterion: kinematics rather than column density governs the relative heights of the peaks, at least in the homogeneous media studied so far. The peak separation and no underlying absorption appear to trace LyC escaping from galaxies better than the EWb/EWr ratio, although these correlations have to be studied on a bigger sample.

4.2. Comparison with GPs and LBAs

Finally, we examine the various quantities that characterise the Lyα profiles as a function of the Lyα equivalent width, which also enables us to include the comparison samples. The results are presented in Fig. 6. For all samples, we see the same trends between the peak separations and EW(Lyα), and between the blue peak location and EW(Lyα), which is in agreement with the correlations presented above: EW(Lyα) vs. $f_{\rm esc}^{\rm LyC}$ (Fig. 2 left), and peak separation/blue peak location vs. $f_{\rm esc}^{\rm LyC}$ (Fig. 5). Only objects with high EWs have small peak separations $V_{\rm sep}$. Although no direct measurements of $f_{\rm esc}^{\rm LyC}$ are available for the comparison sample, some of the objects share all the Lyα characteristics of our LCEs: a strong EW(Lyα) (>70 Å), a high $f_{\rm esc}^{\rm Ly\alpha}$(>20%), a small peak separation, and the whole Lyα profile in emission. This comparison suggests that a fraction of the GP and LBA samples shown here may also be strong ($f_{\rm esc}^{\rm LyC} >$ 5%) LCEs.

5. Discussion

5.1. The lack of underlying absorption

As shown in Fig. 7, a stack of the Lyα profiles of our LCEs over a broad wavelength range (thin blue curve) shows no/weak underlying absorption. This is a very unusual feature. LARS galaxies, which are selected for their strong Hα to trace recent star formation, often have Lyα in absorption, and when in emission, this is usually broad, redshifted, asymmetric, and lying on top of a broad absorption feature (see also Wofford et al. 2013). As an illustration, we overplot the Lyα spectrum of LARS05 (thick black curve), a strong LAE studied in details in Duval et al. (2016). The underlying absorption is clearly visible for this object, especially in the red wing. LARS05 is a galaxy where we do not expect LyC leakage: in Duval et al. (2016), they fit the underlying absorption trough and estimate $N_{\rm HI} \sim 4 \times 10^{20}$ cm^{-2}. We also notice that some objects presented in Alexandroff et al. (2015, Fig. 8), e.g. J1416+1223 or J1414+0540, present a broad absorption feature and are probably not good candidates for LyC escape. The LCE from Borthakur et al. (2014) discussed above, J0921+4509, is presented in the same figure, and its underlying absorption is less pronounced. Our LCEs resemble more closely the objects with no underlying absorption as, for example, J0926+4427 (which is also the GP LARS14).

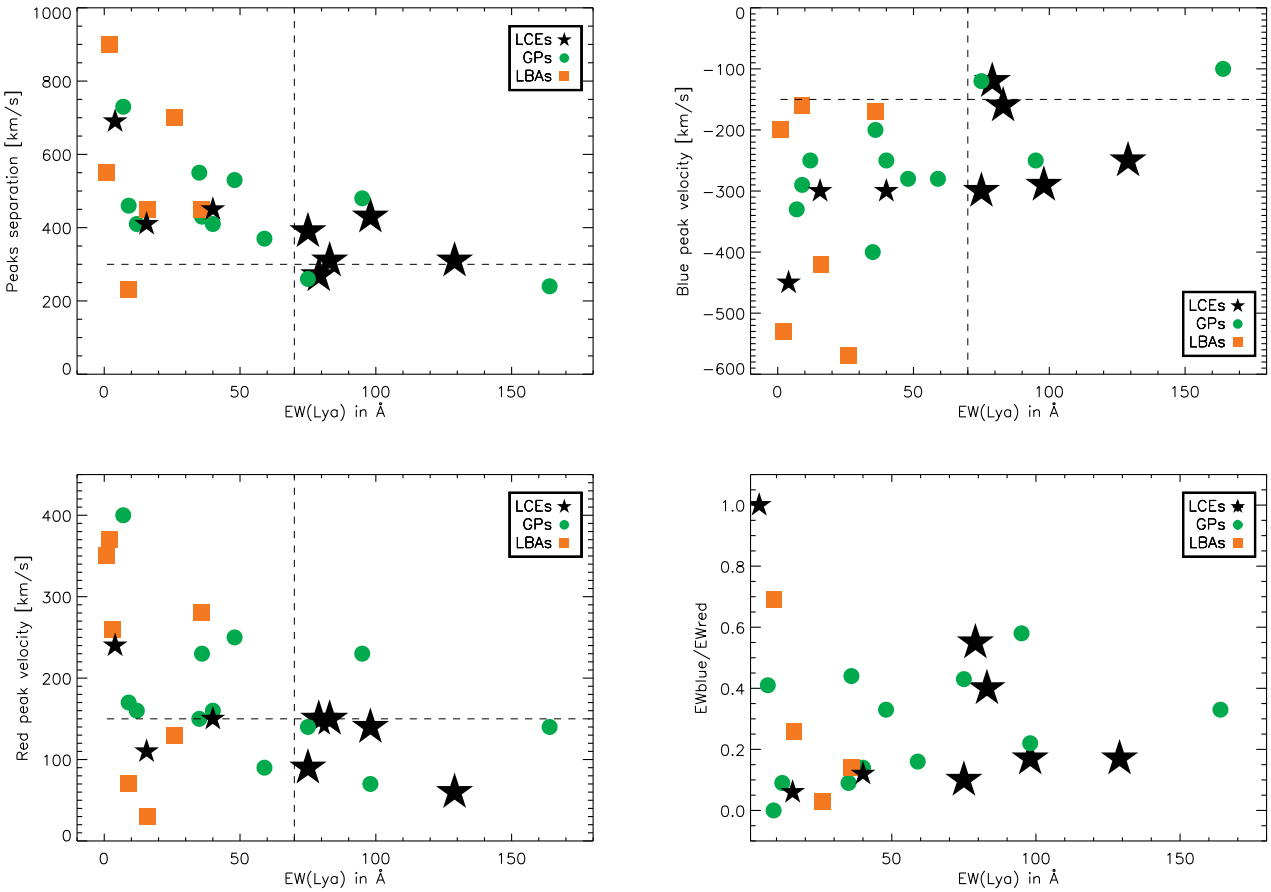

Fig. 6. Comparison of the Lyα diagnostics for LyC leakage over the comparison samples of LBAs and GPs with the same measurements on LCEs. The dashed lines correspond to the theoretical predictions for $f_{\rm esc}^{\rm LyC} \sim 30\%$ ($\tau_{\rm LyC} \sim 1$) from Verhamme et al. (2015). Black stars, green circles, and orange squares show the data of the LCE, GP, and LBA samples, respectively.

The origin of the broad absorption around Lyα can be either stellar or interstellar. For starbursts with ages above ~10 Myr or constant star formation history, synthetic stellar spectra show an absorption around Lyα (e.g. Fig. 2 in Schaerer & Verhamme 2008; Peña-Guerrero & Leitherer 2013). The fact that we don't see this feature in any of our LCEs is consistent with the very young age of their bursts, as determined by SED fitting (Izotov et al. 2016b). But it also means that the interstellar medium is transparent enough not to imprint any visible wing from the Lorentzian profile.

The underlying absorption seen in most Lyα spectra (e.g. LARS and eLARS, or Figs. 4–9 in Wofford et al. 2013) is often broader that the stellar absorption. This is likely due to interstellar absorption: the spectrum emerging from a star-forming region, i.e. the UV stellar continuum plus a nebular Lyα recombination line is absorbed by the interstellar gas along the line of sight, imprinting a Voigt profile on the transmitted[1] stellar UV continuum. This profile, which usually has very broad wings for typical column densities of the ISM (~±6000 km s^{-1} for $N_{\rm HI} \sim 10^{21}$ cm^{-2}), is centered on the bulk velocity of the scattering medium. The central part of the trough on the transmitted spectrum is partially refilled by the resonant Lyα emission, but the spectral shift/broadening owing to radiation transfer through the ISM is usually smaller than the width of the Voigt profile and the wings are still visible in the emergent spectrum. Our spectra do not show any sign of absorption below the Lyα line, except for J1333+6246, which may have some absorption bluewards. The absence of the absorption is a model-independent indication for low column density of neutral gas in front of the UV source, along the line of sight: the Voigt profiles of the absorbing gas along the line of sight are narrower than the wings of the scattered emission components. As discussed above, $f_{\rm esc}^{\rm LyC}$ correspond to $N_{\rm HI} = (3.2\text{–}4.6) \times 10^{17}$ cm^{-2} for our LCEs.

The presence of an underlying absorption in the Lyα spectra of typical star-forming galaxies of the local Universe is certainly enhanced by an aperture effect. LBAs, LARS, and especially eLARS galaxies are closer in redshifts and spatially more extended than typical GPs and our compact LCEs. The COS aperture only partially captures the Lyα emission from these galaxies, as is well demonstrated in Hayes et al. (2013, 2014). The transmitted Lyα spectrum is the same as long as the source is inside the COS aperture, but the scattered component escapes the galaxy over a broad area, which extends over the COS aperture for local starbursts, but may still fall into the detector for these very compact sources.

In summary, our LCEs do not show the usual broad absorption below the Lyα line, probably for a combination of the three reasons proposed above: their bursts are very young and still in the regime where O stars dominate the stellar population, so there is no stellar absorption; their ISM is very transparent along the line of sight: since ionizing radiation escapes, there is no additional interstellar absorption; they are so compact that probably most of the scattered component of the Lyα emission is recovered inside the COS aperture, which refills absorption, if

[1] Photons escaping the medium without scattering constitute the transmitted spectrum.

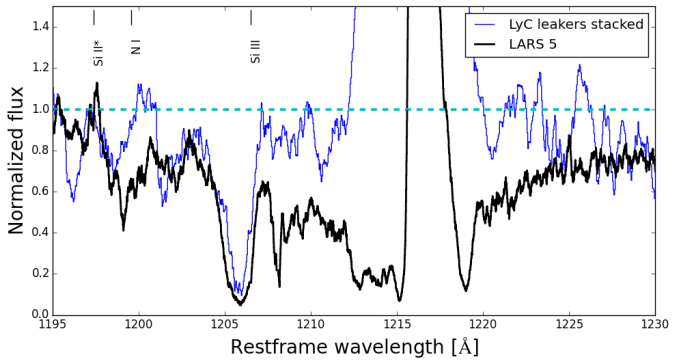

Fig. 7. Comparison of the amount of underlying absorption below the Lyα emission between a stacked spectrum of our five LCEs (thin blue curve) and LARS05 (thick black curve), chosen as representative of typical Lyα profiles in local galaxies: the leakers clearly have less underlying absorption. See text for more details.

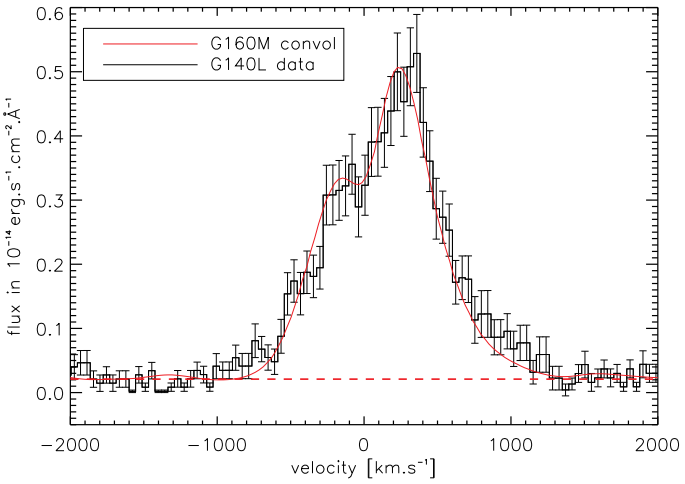

Fig. 8. Lyα spectrum of J1152+3400 in the G140L spectrum, $R \sim 1000$, comparable to high-redshift surveys data for LAEs.

any. More data are needed to determine if these properties are universal of LCEs: are all bursts in LCEs especially young and compact? Can we find some objects emitting ionizing radiation, and with a detectable broad absorption component inside the Lyα emission? Or can we use the presence/absence of underlying absorption as an independent probe of LyC leakage? One LyC detection has been reported so far from a $z \sim .83$ galaxy with Lyα in absorption (Vanzella et al. 2010), which is unexpected from radiation transfer modelling, and given the results of the actual study. If the LyC detection is confirmed further in this interesting object, it will become a great challenge for further theoretical investigations.

5.2. Applicability to high-redshift observations

5.2.1. Effect of a lower spectral resolution

With the exception of few lensed galaxies at $z \sim 3$ observed with $R \sim 5000$ (Fosbury et al. 2003; Vanzella et al. 2016a), Lyα spectra of high redshift galaxies do not reach the medium resolution of the HST/COS G160M grisms. By way of illustration, we show in Fig. 8 the G140L Lyα profile of our strongest leaker, J1152+3400, in black. We checked that when we degrade the G160M spectrum (with an effective resolution of $R \sim 4000$) to qualitatively match the effective spectral resolution of G140L for this object, which is estimated at $R \sim 1000$, we find a similar alteration of the profile, as shown by the red curve in Fig. 8. The dip between the peaks is not visible anymore in the low resolution data, the peaks are barely resolved. Indeed, the peak separation is $V_{\rm sep} = 270$ km s^{-1} for this object, just below $\Delta V \sim 300$ km s^{-1}, which corresponding with a resolving power of $R = 1000$. We tested on the G140L data how the EWs and velocity shifts are altered by low spectral resolution. We did the same measurements on the G140L spectra of our five leakers and found that we recover EW(Lyα) of the G160M measurements within the uncertainties of the continuum level estimation, but the velocity shifts are more strongly affected, up to hundreds of km s^{-1}, depending on the spectral shape. This implies that a spectral resolution of $R \gtrsim 1000$ is needed to measure the smallest peak separation that is typical of strong LCEs: the Lyα spectra of LCEs in these surveys should appear as strong and narrow single peaked spectra. If the double peaks are resolved, it means that $V_{\rm sep}$ is too large to trace strong LyC escape.

5.2.2. Effect of IGM attenuation

The neutral fraction of the IGM increases with redshift (Madau 1995) and alters the transmission of high-redshift Lyα spectra (e.g. Haiman 2002; Santos 2004; Dijkstra 2014). For example, Laursen et al. (2011) show how the blue part of the Lyα line can, in hydrodynamical simulations of galaxy formation, be scattered out of the line of sight of high redshift galaxies by neutral gas along the way, which alters the synthetic Lyα profile shapes. Observations also witness a sudden transition in the evolution of the Lyα properties of galaxies with redshift: the fraction of Lyα emitting galaxies among LBGs increases regularly with redshift, up to $z \sim 6$, where a sharp decrease is observed (e.g. Schenker et al. 2014). The same behaviour has been reported for the evolution of $f_{\rm esc}^{\rm Ly\alpha}$ with redshift (Hayes et al. 2011). However IGM attenuation is a very stochastic process and greatly varies from line of sight to line of sight (Inoue et al. 2014). Maybe for that reason, a significant fraction of double-peaked Lyα emitters have still been observed at intermediate redshifts ($z \sim 2$–3), where the mean IGM transmission fraction is 30% (Inoue et al. 2014) among LBG and LAE populations (Kulas et al. 2012; Yamada et al. 2012; Hashimoto et al. 2015), some with particularly small peaks separation (Vanzella et al. 2016a). Generally, the blue part of Lya emission has an increasing chance of being decreased (washed out) at high-z, which means that detecting multiple peaks and measuring separation will, on average, become more difficult at high-z. However, for galaxies located in large ionized bubbles, as recently found by Castellano et al. (2016), and suggested by Matthee et al. (2015), this may not be a problem.

Our actual sample of local LCEs enables us to calibrate diagnostics for LyC leakage from Lyα properties. If LAEs with strong double-peaked Lyα profiles and small separation are still detected at the highest redshift, they will be the best candidates for the sources of reionization, and may put constraints on the patchiness of reionization processes.

5.3. Comparison of Lyα and [O III]/[O II] diagnostics for LyC escape

As discussed above, high [O III]/[O II] ratios have been proposed for tracing density-bound H II regions in galaxies (Jaskot & Oey 2013; Nakajima & Ouchi 2014). Our five LCEs were selected

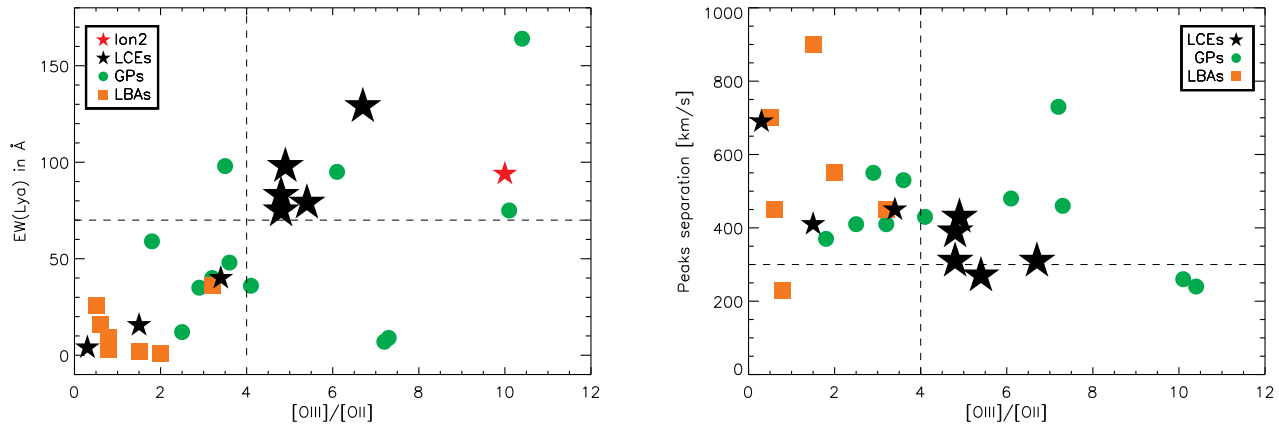

Fig. 9. Comparison of the Lyα diagnostics for LyC leakage with [O III]/[O II] ratios.

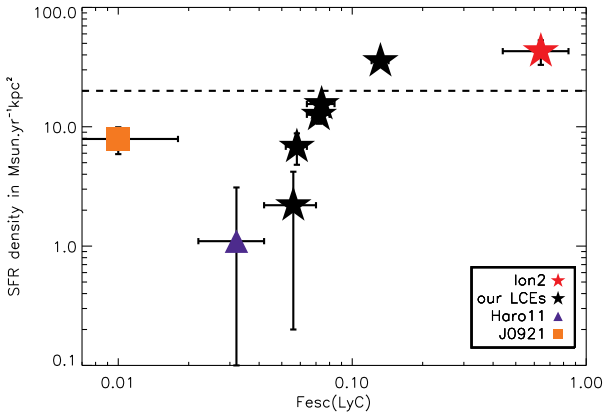

Fig. 10. Correlation between $f_{\rm esc}^{\rm LyC}$ and the SFR surface density. Same symbols as in Fig. 1.

for their high [O III]/[O II] ratios (and compactness), they all leak ionizing radiation (Izotov et al. 2016a,b), and we have just shown that they also have peculiar Lyα properties (EW(Lyα) > 70 Å and a small peak separation), in line with our theoretical predictions (Verhamme et al. 2015). So we naturally find correlations between the [O III]/[O II] ratios of LCEs and EW(Lyα) or $V_{\rm sep}$, as illustrated in Fig. 9. But we also see in this figure that applying both criteria for LyC leakage to the comparison sample of galaxies can help to select the best follow-up targets. From this exercise, three GPs (J1219+1526 and J1424+4217 from Henry et al. 2015; and J0815+2156 from Jaskot & Oey 2014) appear as very probable LCEs, fulfilling both criteria.

5.4. What physical processes make these galaxies leak ionizing photons ?

We demonstrated above that Lyα and [O III]/[O II] are useful diagnostics to infer LyC leakage from galaxies, or to select good LCE candidates, because both can trace a low density path through the interstellar medium of galaxies along the line of sight. But these measurements do not explain the physical reason for the existence of low density paths through our galaxies.

Our five LCEs are extremely compact, undergoing a strong star formation episode, so they have particularly high SFR surface densities, Σ_{SFR}. This has been proposed as a mechanism for the escape of LyC photons (Heckman et al. 2011; Sharma et al. 2016). Indeed, we find a strong correlation between Σ_{SFR} and the escape fraction of ionizing radiation from galaxies, $f_{\rm esc}^{\rm LyC}$, as shown in Fig. 10. We interpret this correlation as a good indication that concentrated star formation is necessary for LyC escape, either by producing a lot of ionizing radiation from a concentration of young stars, photoionizing the ISM (the so-called density-bound scenario), or by mechanical feedback from these young stars (stellar winds, radiation pressure, supernova creating holes along random sight-lines), or both.

6. Conclusions

We have analysed the properties of the Lyα line of five low-redshift Lyman continuum leaking galaxies that were observed with the COS spectrograph onboard HST that have recently been reported by Izotov et al. (2016a,b). The $z \sim 0.3$ sources were selected for compactness and for showing a high emission line ratio [O III]/[O II] that has previously been proposed as a possible diagnostic for Lyman continuum escape (Jaskot & Oey 2013; Nakajima & Ouchi 2014). For comparison, we have also included the other confirmed low-z LCEs, and HST/COS observations from samples of GP galaxies and LBAs, which have been suggested to be LCEs (see Sect. 2). We have presented the behaviour of the Lyα equivalent width, EW(Lyα), the Lyα escape fraction ($f_{\rm esc}^{\rm Ly\alpha}$), and several measures of the Lyα line profile, and discussed how these quantities depend on the Lyman continuum escape fraction, $f_{\rm esc}^{\rm LyC}$.

We found that strong LCEs, defined by an escape fraction $f_{\rm esc}^{\rm LyC} > 5\%$, are characterised by strong Lyα emission, as measured by EW(Lyα) and $f_{\rm esc}^{\rm Ly\alpha}$. Furthermore, their Ly$\alpha$ line profiles show a double-peak structure with two emission peaks that are blue- and redward of the central wavelength with a small separation between the peaks ($V_{\rm sep} \sim 300-400$ km s^{-1}). This confirms qualitatively the predictions of Verhamme et al. (2015) from radiation transfer models. More precisely, our main results can be summarised as follows:

- All strong LCEs show EW(Lyα) > 70 Å and $f_{\rm esc}^{\rm Ly\alpha} > 0.2$, suggesting that these quantities could be used as efficient selection criteria to find potential sources (or analogs) of cosmic reionization (see Fig. 1).
- The restframe EW(Lyα) increases with the Lyman continuum escape fraction and reaches EW(Lyα) $\sim$ 70–130 Å (Fig. 2 left).
- Empirically the Lyα escape fraction correlates with the Lyman continuum escape fraction (Fig. 2 right). On average $f_{\rm esc}^{\rm Ly\alpha}/f_{\rm esc}^{\rm LyC} \sim 2-3$, indicating that Ly$\alpha$ photons escape more

efficiently than the ionizing photons, as expected because of radiation transfer effects (Sect. 3).
- The separation between the blue and red peaks decreases with increasing $f_{\rm esc}^{\rm LyC}$, as expected for decreasing HI column densities (Verhamme et al. 2015). Whereas the red peak of most LCEs is $V_{\rm peak}^{\rm red} \sim 80-150$ km s^{-1}, the blue peak can be shifted by larger amounts ($V_{\rm peak}^{\rm blue} \sim -300$ to -150 km s^{-1}). The shift of the blue peak is found to correlate with $f_{\rm esc}^{\rm LyC}$ (Fig. 5).
- No clear correlation is found for LCEs between the ratio of the blue and red equivalent widths and $f_{\rm esc}^{\rm LyC}$.
- A comparison of the Lyα line properties of GPs and LBAs with those of the LCEs shows that a subset of these galaxies could indeed be emitters in the Lyman continuum (see Fig. 6).
- We find a correlation between $f_{\rm esc}^{\rm LyC}$ and the SFR surface density (see Fig. 10), indicating that the compactness of star-forming regions could play a significant role in shaping low density channels through the ISM of LCEs.

Although larger samples of LCEs are needed to establish more robust correlations between Lyman continuum escape and other properties, the observations reported here should provide useful guidance to find and more efficiently select the sources of cosmic reionization or their analogs.

Acknowledgements. We thank Max Gronke for stimulating discussions and for sharing his simulation data. A.V. thanks Mirka Dessauges for useful discussion about data reduction and spectral measurements. A.V. is supported by a Marie Heim Vögtlin fellowship of the Swiss National Foundation. IO acknowledges the support from the grant 14-20666P of Czech Science Foundation, together with the long-term institutional grant RVO:67985815. Based on observations made with the NASA/ESA *Hubble* Space Telescope, obtained from the data archive at the Space Telescope Science Institute. Support for this work was provided by NASA through grant number HST-GO-13744.001-A from the STScI. All of the HST data presented in this paper were obtained from the Mikulski Archive for Space Telescopes (MAST). STScI is operated by the Association of Universities for Research in Astronomy, Inc., under NASA contract NAS5-26555. Support for MAST for non-HST data is provided by the NASA Office of Space Science via grant NNX13AC07G and by other grants and contracts. We made use of the SAO/NASA Astrophysics Data System (ADS), the NASA/IPAC Extragalactic Database (NED), and the Image Reduction and Analysis Facility (IRAF), distributed by the National Optical Astronomy Observatories. Based on observations made with the NASA/ESA *Hubble* Space Telescope, obtained [from the Data Archive] at the Space Telescope Science Institute, which is operated by the Association of Universities for Research in Astronomy, Inc., under NASA contract NAS 5-26555. These observations are associated with program 13744.

References

Alexandroff, R. M., Heckman, T. M., Borthakur, S., Overzier, R., & Leitherer, C. 2015, ApJ, 810, 104
Atek, H., Kunth, D., Hayes, M., Östlin, G., & Mas-Hesse, J. M. 2008, A&A, 488, 491
Atek, H., Kunth, D., Schaerer, D., et al. 2014, A&A, 561, A89
Behrens, C., Dijkstra, M., & Niemeyer, J. C. 2014, A&A, 563, A77
Bergvall, N., Zackrisson, E., Andersson, B.-G., et al. 2006, A&A, 448, 513
Borthakur, S., Heckman, T. M., Leitherer, C., & Overzier, R. A. 2014, Science, 346, 216
Cardamone, C., Schawinski, K., Sarzi, M., et al. 2009, MNRAS, 399, 1191
Castellano, M., Dayal, P., Pentericci, L., et al. 2016, ApJ, 818, L3
de Barros, S., Vanzella, E., Amorín, R., et al. 2016, A&A, 585, A51
Dijkstra, M. 2014, PASA, 31, 040
Dijkstra, M. 2016, in Astrophys. Space Sci. Lib. 423, ed. A. Mesinger, 145
Dijkstra, M., Gronke, M., & Venkatesan, A. 2016, ApJ, 828, 71
Dopita, M. A., & Sutherland, R. S. 2003, Astrophysics of the Diffuse Universe, Astron. Astrophys. Lib. (Springer)
Duval, F., Östlin, G., Hayes, M., et al. 2016, A&A, 587, A77
Erb, D. K., Steidel, C. C., Trainor, R. F., et al. 2014, ApJ, 795, 33
Fontanot, F., Cristiani, S., & Vanzella, E. 2012, MNRAS, 425, 1413
Fontanot, F., Cristiani, S., Pfrommer, C., Cupani, G., & Vanzella, E. 2014, MNRAS, 438, 2097
Fosbury, R. A. E., Villar-Martín, M., Humphrey, A., et al. 2003, ApJ, 596, 797
Giallongo, E., Grazian, A., Fiore, F., et al. 2015, A&A, 578, A83
Gronke, M., & Dijkstra, M. 2016, ApJ, 826, 14
Haiman, Z. 2002, ApJ, 576, L1
Hashimoto, T., Verhamme, A., Ouchi, M., et al. 2015, ApJ, 812, 157
Hayes, M., Schaerer, D., Östlin, G., et al. 2011, ApJ, 730, 8
Hayes, M., Östlin, G., Schaerer, D., et al. 2013, ApJ, 765, L27
Hayes, M., Östlin, G., Duval, F., et al. 2014, ApJ, 782, 6
Heckman, T. M., Hoopes, C. G., Seibert, M., et al. 2005, ApJ, 619, L35
Heckman, T. M., Borthakur, S., Overzier, R., et al. 2011, ApJ, 730, 5
Henry, A., Scarlata, C., Martin, C. L., & Erb, D. 2015, ApJ, 809, 19
Inoue, A. K., Shimizu, I., Iwata, I., & Tanaka, M. 2014, MNRAS, 442, 1805
Izotov, Y. I., Guseva, N. G., & Thuan, T. X. 2011, ApJ, 728, 161
Izotov, Y. I., Orlitová, I., Schaerer, D., et al. 2016a, Nature, 529, 178
Izotov, Y. I., Schaerer, D., Thuan, T. X., et al. 2016b, MNRAS, 461, 3683
Jaskot, A. E., & Oey, M. S. 2013, ApJ, 766, 91
Jaskot, A. E., & Oey, M. S. 2014, ApJ, 791, L19
Kulas, K. R., Shapley, A. E., Kollmeier, J. A., et al. 2012, ApJ, 745, 33
Laursen, P., Sommer-Larsen, J., & Razoumov, A. O. 2011, ApJ, 728, 52
Leitet, E., Bergvall, N., Piskunov, N., & Andersson, B.-G. 2011, A&A, 532, A107
Leitet, E., Bergvall, N., Hayes, M., Linné, S., & Zackrisson, E. 2013, A&A, 553, A106
Leitherer, C., Hernandez, S., Lee, J. C., & Oey, M. S. 2016, ApJ, 823, 64
Madau, P. 1995, ApJ, 441, 18
Madau, P., & Haardt, F. 2015, ApJ, 813, L8
Matthee, J., Sobral, D., Santos, S., et al. 2015, MNRAS, 451, 400
Matthee, J., Sobral, D., Best, P., et al. 2016a, MNRAS, submitted [arXiv:1605.08782]
Matthee, J., Sobral, D., Oteo, I., et al. 2016b, MNRAS, 458, 449
Micheva, G., Iwata, I., & Inoue, A. K. 2016, MNRAS, submitted [arXiv:1604.00102]
Nakajima, K., & Ouchi, M. 2014, MNRAS, 442, 900
Ocvirk, P., Gillet, N., Shapiro, P. R., et al. 2016, MNRAS, 463, 1462
Östlin, G., Hayes, M., Kunth, D., et al. 2009, AJ, 138, 923
Östlin, G., Hayes, M., Duval, F., et al. 2014, ApJ, 797, 11
Overzier, R. A., Heckman, T. M., Tremonti, C., et al. 2009, ApJ, 706, 203
Peña-Guerrero, M. A., & Leitherer, C. 2013, AJ, 146, 158
Rivera-Thorsen, T. E., Hayes, M., Östlin, G., et al. 2015, ApJ, 805, 14
Santos, M. R. 2004, MNRAS, 349, 1137
Schaerer, D. 2003, A&A, 397, 527
Schaerer, D., & Verhamme, A. 2008, A&A, 480, 369
Schenker, M. A., Ellis, R. S., Konidaris, N. P., & Stark, D. P. 2014, ApJ, 795, 20
Shapley, A. E., Steidel, C. C., Pettini, M., & Adelberger, K. L. 2003, ApJ, 588, 65
Shapley, A. E., Steidel, C. C., Strom, A. L., et al. 2016, ApJ, 826, L24
Sharma, M., Theuns, T., Frenk, C., et al. 2016, MNRAS, 458, L94
Stark, D. P., Ellis, R. S., & Ouchi, M. 2011, ApJ, 728, L2
Steidel, C. C., Bogosavljević, M., Shapley, A. E., et al. 2011, ApJ, 736, 160
Syphers, D., Anderson, S. F., Zheng, W., et al. 2012, AJ, 143, 100
Vanzella, E., Giavalisco, M., Inoue, A. K., et al. 2010, ApJ, 725, 1011
Vanzella, E., de Barros, S., Castellano, M., et al. 2015, A&A, 576, A116
Vanzella, E., De Barros, S., Cupani, G., et al. 2016a, ApJ, 821, L27
Vanzella, E., de Barros, S., Vasei, K., et al. 2016b, ApJ, 825, 41
Vasei, K., Siana, B., Shapley, A. E., et al. 2016, ApJ, submitted [arXiv:1603.02309]
Verhamme, A., Orlitová, I., Schaerer, D., & Hayes, M. 2015, A&A, 578, A7
Wofford, A., Leitherer, C., & Salzer, J. 2013, ApJ, 765, 118
Worseck, G., Prochaska, J. X., McQuinn, M., et al. 2011, ApJ, 733, L24
Yamada, T., Matsuda, Y., Kousai, K., et al. 2012, ApJ, 751, 29
Yang, H., Malhotra, S., Gronke, M., et al. 2016, ApJ, 820, 130
Zackrisson, E., Inoue, A. K., & Jensen, H. 2013, ApJ, 777, 39